THE JOURNAL OF BIOLOGICAL CHEMISTRY
Vol. 279, No. 22, Issue of May 28, pp. 23504–23509, 2004
Printed in U.S.A.

Crystal Structure of Kinesin Regulated by Ca^{2+}-Calmodulin*

Received for publication, January 22, 2004, and in revised form, February 18, 2004
Published, JBC Papers in Press, February 26, 2004, DOI 10.1074/jbc.M400741200

Maia V. Vinogradova‡, Vaka S. Reddy§, Anireddy S. N. Reddy§, Elena P. Sablin‡, and Robert J. Fletterick‡¶

From the ‡Department of Biochemistry/Biophysics, University of California, San Francisco, California 94143-2240 and §Department of Biology and Program in Cell and Molecular Biology, Colorado State University, Fort Collins, Colorado 80523

Kinesins orchestrate cell division by controlling placement of chromosomes. Kinesins must be precisely regulated or else cell division fails. Calcium, a universal second messenger in eukaryotes, and calmodulin regulate some kinesins by causing the motor to dissociate from its biological track, the microtubule. Our focus was the mechanism of calcium regulation of kinesin at atomic resolution. Here we report the crystal structure of kinesin-like calmodulin-binding protein (KCBP) from potato, which was resolved to 2.3 Å. The structure reveals three subdomains of the regulatory machinery located at the C terminus extension of the kinesin motor. Calmodulin that is activated by Ca^{2+} ions binds to an α-helix positioned on the microtubule-binding face of kinesin. A negatively charged segment following this helix competes with microtubules. A mimic of the conventional kinesin neck, connecting the calmodulin-binding helix to the KCBP motor core, links the regulatory machine to the kinesin catalytic cycle. Together with biochemical data, the crystal structure suggests that Ca^{2+}-calmodulin inhibits the binding of KCBP to microtubules by blocking the microtubule-binding sites on KCBP.

Calcium ions regulate many physiological processes. Calmodulin, a highly conserved, multifunctional Ca^{2+}-binding protein, mediates a majority of the calcium-regulated processes and functions as a key transducer of changes in cytosolic calcium (1). Activated by calcium ions, calmodulin interacts with functionally diverse proteins and regulates their activities and functions. Calmodulin or other calmodulin-like calcium sensors are required for structural integrity, regulation of actin-based myosin and microtubule (MT)[1]-based dynein (2, 3), motor proteins involved in muscle contraction, cell division, and organelle transport. Kinesins, which are microtubule-based motor proteins, control developmental and cellular processes in eukaryotes (4–6). The molecular basis of Ca^{2+}-calmodulin regulation has been described for kinesin-like calmodulin-binding protein (7–9). Kinesin-like calmodulin-binding protein (KCBP), a member of the Ncd subfamily of minus end-directed kinesin motor proteins (8) found in all plants and in some animals (10), is required for cell division and trichome morphogenesis (11–13). Biochemical studies show that Ca^{2+}-activated calmodulin disrupts interactions between KCBP and microtubules and, therefore, controls the motility of the motor, microtubule-stimulated ATPase activity, and microtubule bundling properties (14, 15). The Ca^{2+}-dependent regulation of KCBP is conferred by a calmodulin-binding motif at the C-terminal extension of the motor core (16, 17). We crystallized and then determined the three-dimensional structure of the KCBP motor core with the associated calmodulin regulatory motif to better understand the regulation of kinesins, and the mechanism of Ca^{2+} signal transduction by calmodulin.

EXPERIMENTAL PROCEDURES

Materials—pET28b vector and *Escherichia coli* BL21(DE3) were from Novagen. ATP was purchased from Sigma. Calmodulin-Sepharose 4B was from Amersham Biosciences. Crystallization screens were from Hampton Research. All other chemicals were of reagent grade.

Preparation and Crystallization of the Recombinant KCBP—The potato KCBP cDNA fragment encoding amino acid residues Glu^{884}–Glu^{1252} was synthesized by PCR using a cDNA template (GenBank™ accession no. L46702) with forward (5′-GCATGCCATGGAAGATATGAAAGGCAAG-3′) and reverse (5′-GCAGAATTCATTCGTCTTGGATTTCCT-3′) primers. The amplified PCR product was digested with NcoI-EcoRI and ligated into NcoI-EcoRI sites in pET28b vector. The recombinant vector was verified by sequencing and transformed into BL21(DE3) *E. coli* cells for protein expression. The recombinant KCBP containing the motor core (amino acids 884–1208) with the C-terminal extension (amino acids 1209–1252), including the calmodulin-binding motif (amino acids 1221–1236), was expressed and purified using a calmodulin-Sepharose 4B column as described (14–16). The purified protein (in 50 mM Tris, pH 7.5, 50 mM NaCl, 2 mM $MgCl_2$, 1 mM EGTA, 1 mM ATP, 1 mM Tris(2-carboxyethyl)-phosphine) was concentrated to 10 mg/ml and used fresh for crystallization experiments. The recombinant KCBP was crystallized at +4 °C using the sitting drop vapor diffusion method and 20% polyethylene glycol 3350 in 0.2 M di-sodium hydrogen phosphate, pH 9.1, as the reservoir solution. Before x-ray data collection, the crystals were transferred into a cryoprotecting solution containing 15% polyethylene glycol 400 in the reservoir solution and were then flash-frozen in liquid nitrogen.

Data Collection, Model Building, and Refinement—X-ray diffraction data were collected at Advanced Light Source (Lawrence Berkeley National Laboratory) beamline 8.3.1. (λ = 1.1 Å), processed using DENZO, and scaled by SCALEPACK (18). The structure of KCBP was determined by molecular replacement (crystallography NMR software (19)) using atomic coordinates for the motor domain of human kinesin (PDB entry 1MKJ). Electron density maps based on coefficients $2F_o - F_c$ were calculated from the phases of the initial model. The refinement was carried out using the crystallography NMR software and alternating with manual rebuilding steps using QUANTA (Accelrys). The entire structure was checked and rebuilt using annealed omit maps and PROCHECK script from a CCP4 package (20). The current crystallographic model is refined to 2.3 Å, with R/R_{free} values of 21.2/25.4, and contains 344 visible amino acid residues, 121 water molecules, and one Mg^{2+}-

* This work was supported by National Institutes of Health Grant PO1 AR42895 and a National Science Foundation Grant (to A. S. N. R.). The costs of publication of this article were defrayed in part by the payment of page charges. This article must therefore be hereby marked "*advertisement*" in accordance with 18 U.S.C. Section 1734 solely to indicate this fact.

The atomic coordinates and structure factors (code 1SDM) have been deposited in the Protein Data Bank, Research Collaboratory for Structural Bioinformatics, Rutgers University, New Brunswick, NJ (http://www.rcsb.org/).

¶ To whom correspondence should be addressed. Tel.: 415-476-5080; Fax: 415-476-1902; E-mail: flett@msg.ucsf.edu.

[1] The abbreviations used are: MT, microtubule; KCBP, kinesin-like calmodulin-binding protein; PDB, Protein Data Bank; Ncd, non-claret disjunction; AMPPCP, adenosine 5′-(β,γ-methylene)triphosphate.

ADP complex. There was no visible electron density for five N-terminal amino acid residues (884–888), a loop L11 segment (residues 1126–1134), and part of the C-terminal region (residues 1234–1244).

RESULTS

Structure of KCBP, General and Specific Features—In crystallization trials we used recombinant KCBPs from different species including *Arabidopsis*, maize, spruce, and potato. The monomeric potato KCBP Glu^{884}–Glu^{1252} produced crystals suitable for determining the structure at a high resolution. Table I shows x-ray data collection and refinement statistics. The crystal structure of KCBP shows that the motor core of this plant kinesin shares overall similarity to animal and human analogues (21–24) (Fig. 1*A*). Electron density corresponding to Mg^{2+}-ADP is seen in the nucleotide binding pocket. Fig. 1, *B* and *C*, shows that the positions of α-helices and β-strands in the motor core match the positions of their counterparts in the structures of Ncd (22) and human conventional kinesin (23). The main differences are found in the positions and the lengths of several surface loops.

TABLE I
Data collection and refinement statistics

Space group	$P2_12_12$
Unit cell (Å)	a = 95.728, b = 85.302, c = 44.457
Data collection	
Resolution (Å)	2.3
Unit reflections	15,165
Observed reflections	340,742
Completeness (%)	90.3
R_{sym} (%)	5.1
$\langle I\rangle/\langle\sigma\ (I)\rangle$	18.96
Refinement (25–2.3 Å)	
R_{cryst} (%)	21.2
R_{free} (%)	25.4
r.m.s.[a] deviation from ideality	
Bonds (Å)	0.008
Angles (°)	1.4
Average *B*-factor (Å^2)	34.3
Molecules per asymmetric unit	1

[a] r.m.s., root mean square.

The structure of KCBP reveals the C-terminal extension of the motor core. This extension was not revealed in the structures of C-terminal kinesins (Kar3 (25), Ncd (22)) or their mutants (26, 27). In KCBP, the C-terminal extension includes the calmodulin-binding helix, two segments with irregular but ordered structures (Fig. 1*A*, *red*), and a fragment with disordered protein chain (Fig. 1*A*, *red dotted line*). The first irregular segment precedes the calmodulin-binding helix and connects it with the motor core; another, rich in negatively charged amino acids (we named it the negative segment), completes the C terminus. An unexpected discovery was that the position of the segment preceding the calmodulin-binding helix is identical to the position of the neck linker in the conventional plus end-directed kinesin (23). The striking similarity in the sequences and interactions holding these linkers along the motor head (Fig. 2*A*) suggests the name "neck mimic" for this segment of the C extension.

At the tip of the arrowhead-shaped motor, the neck mimic and the true conventional kinesin neck take different paths (Fig. 1*C*). As observed in the KCBP structure, the calmodulin-binding helix that follows, although slightly contacting a neighboring motor in the crystal, is positioned by specific contacts within the molecule (Fig. 2*B*) and is likely to be in this approximate location when calmodulin is present. Multiple electrostatic and hydrophobic interactions hold the entire neck mimic and the N-terminal base of the calmodulin-binding helix docked along the motor core. In addition, the extended aliphatic side chain of Lys^{1221}, which is conserved in plant KCBPs, contributes to the limitation of rotational freedom of the helix (Fig. 2*B*). These registrations determine the position of the calmodulin-binding helix and bring it on the kinesin microtubule-binding interface (28).

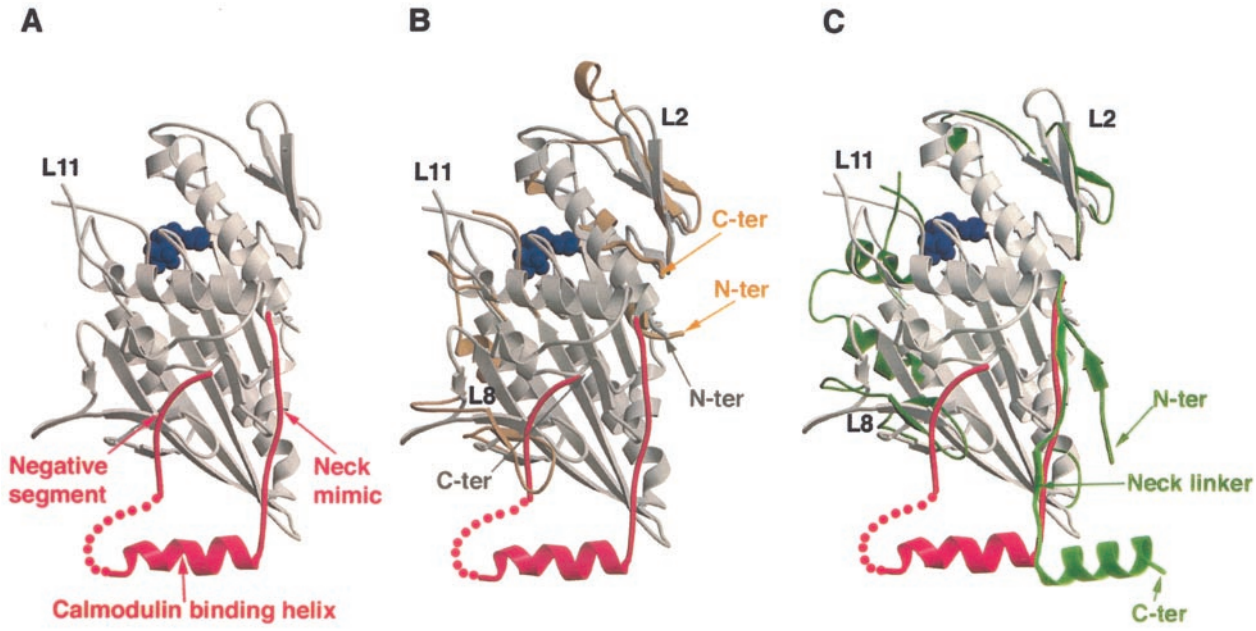

FIG. 1. **The crystal structure and specific features of potato KCBP.** *A*, the polypeptide chain for the KCBP motor core is shown in *gray*. Part of loop L11 is disordered in the KCBP structure and is not shown. Three segments of the C-terminal extension, including the neck mimic (residues 1210–1220), calmodulin-binding helix (residues 1221–1233), and negative coil (residues 1245–1252) are highlighted in *red*. The disordered part of the C-terminal extension is shown as a *red dotted line*. Mg-ADP is shown as a *blue* space-filling model. *B*, superimposition of the KCBP structure with the motor core of *Drosophila* Ncd (22) (residues 349–670; PDB entry 2NCD) using the Cα atoms of the kinesin-conserved nucleotide binding loop, the P loop (amino acids 970–977 and 434–441 in KCBP and Ncd, respectively). The color scheme is consistent with *A* and *C*. Structural elements of Ncd that differ from the KCBP structure are shown in *beige*. *C*, superimposition of KCBP with the structure of human conventional kinesin motor domain (23) (P loop residues, amino acids 86–93; PDB entry 1MJK). Structural elements of kinesin that differ from KCBP are shown in *green*. The kinesin neck linker and part of the neck coiled coil (residues 325–349) are in *bright green*.

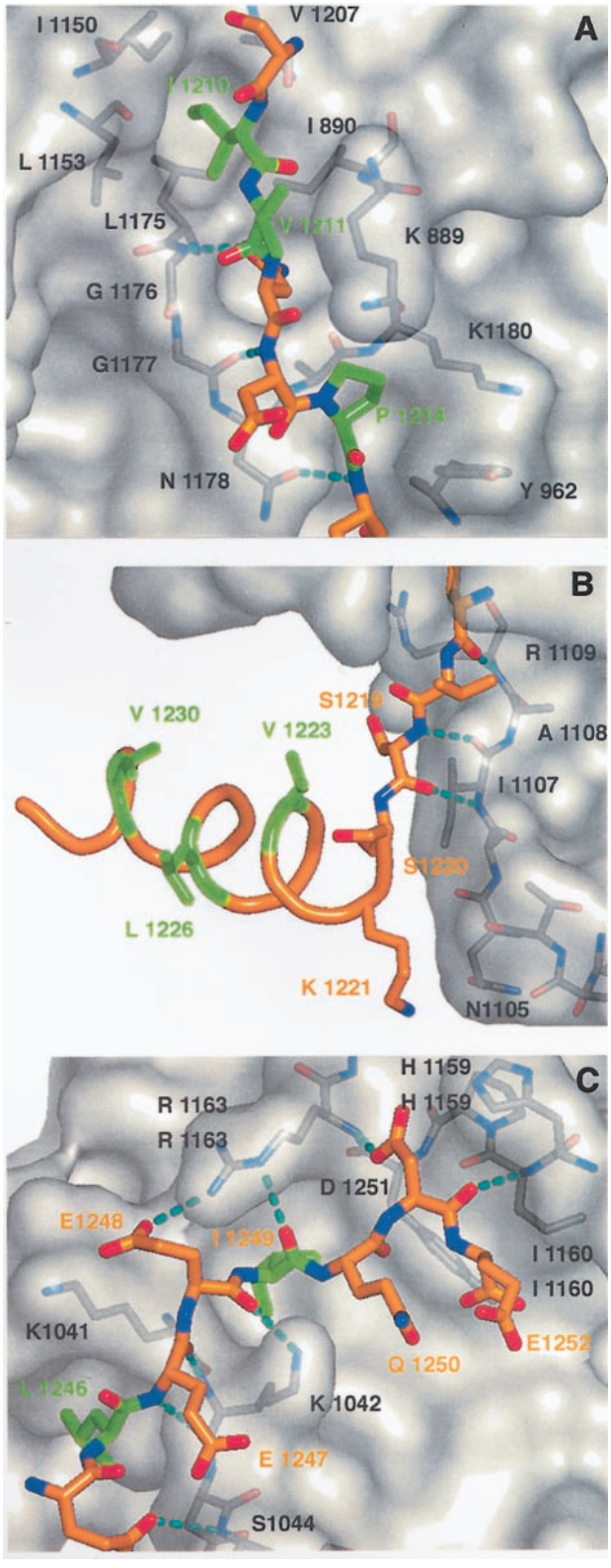

FIG. 2. **The intramolecular contacts defining orientation of the calmodulin-binding domain of KCBP.** Molecular surface of the motor core is in transparent *gray*. Residues of the core interacting with the regulatory C-terminal extension are shown *underneath* the molecular surface in atom coding colors and are indicated in *black*. The C-terminal extension residues are highlighted and indicated: carbon atoms are *orange*; oxygen atoms are *bright red*; and nitrogen atoms are *bright blue*. The hydrophobic residues involved in specific interactions are shown in *green*. *A*, the neck mimic (residues 1210–1220) is docked along the motor core where it is stabilized by specific hydrophobic and electrostatic interactions (hydrogen bonds are shown as *cyan dotted lines*). *B*, the hydrophobic residues in the calmodulin-binding helix implicated in binding with calmodulin are positioned on one face of the helix and are shown in *green*. In the crystal lattice, these residues interact with the equivalent residues from the symmetry-related KCBP molecule. *C*, the C-terminal negative coil is attached to the motor core by multiple hydrogen bonds and is also supported by hydrophobic interactions.

The flexibility of the loop between the calmodulin-binding helix and negative segment does not prevent the negative segment from making extensive contacts with the KCBP motor core (Fig. 2*C*). Analysis of these contacts shows that binding of the negative segment involves residues that are highly conserved in the kinesin motors (including the characteristic HIPYR sequence), which belong to the major microtubule-binding elements, loops L12 and L8, of the motor. Numerous specific electrostatic and hydrophobic contacts (Fig. 2*C*) holding the negative segment on the microtubule-binding face of KCBP exclude the possibility of random interaction and suggest that this segment should be considered part of the regulatory machinery (see "Discussion").

Modeling of KCBP-Calmodulin Complex on Microtubules—Assuming the collapsed conformation of the central helix observed in many structures of calmodulin bound to its peptide targets (29, 30), we built calmodulin into the structure of KCBP (Fig. 3*A*). Modeling shows that the configuration of the calmodulin-binding helix over the microtubule-binding surface of kinesin has roughly enough volume to accommodate a calmodulin molecule without altering the structure of the motor core. The model of calmodulin on KCBP bound to the microtubule (Fig. 3*B*, see figure legend for modeling details) demonstrates that the calmodulin-binding helix in this position is accessible for calmodulin. This observation is consistent with the results of biochemical studies describing dissociation of the preformed KCBP-MT complex in the presence of Ca^{2+}-calmodulin (14). Evidently, bound calmodulin would interfere with loop L8 of the motor core, which is one of the important microtubule-binding elements (28). This interference by itself might be sufficient for detaching the motor from MTs. Additional repelling interactions between calmodulin and tubulin could also arise (Fig. 3*B*) and facilitate the detachment.

Conformational State of KCBP—Remarkably, the structure of KCBP reported here is the first structure of the C-terminal minus end-directed kinesin in the ATP-like conformational state (21–27, 31). To analyze the conformational state of the motor, the structure of KCBP has been superimposed over the structures of kinesins in different structural conformations. The comparison shows that, despite the ADP bound in the nucleotide binding pocket, the major nucleotide-responsive region of the motor (the switch II cluster) is in the ATP-like conformation (31). Fig. 4*A* shows that helices α4 and α5 of the switch II cluster moved closer to the bound nucleotide and match the positions of their counterparts in the previously determined structure of the plus end-directed kinesin KIF1A, complexed with AMPPCP, a nonhydrolyzable analogue of ATP (31). Kinesin motors in the ATP-like conformation, in the absence of γ-phosphate in the nucleotide binding pocket, have been reported (23, 24, 31). In selected structures of rat (24) and human kinesin (23) crystallized with Mg^{2+}-ADP, the switch II cluster elements are configured as in the ATP-like state (21,22, 25–27, 31).

Another nucleotide-responsive element of KCBP, switch I loop L9, is ordered and positioned closer to the bound nucleotide than in any previously determined kinesin structures. The structure of switch I deviates in the available kinesin structures (including those in the ATP-like conformation) suggesting that structuring of switch I loop L9 requires the presence of MTs; however, the resulting tight configuration of the KCBP

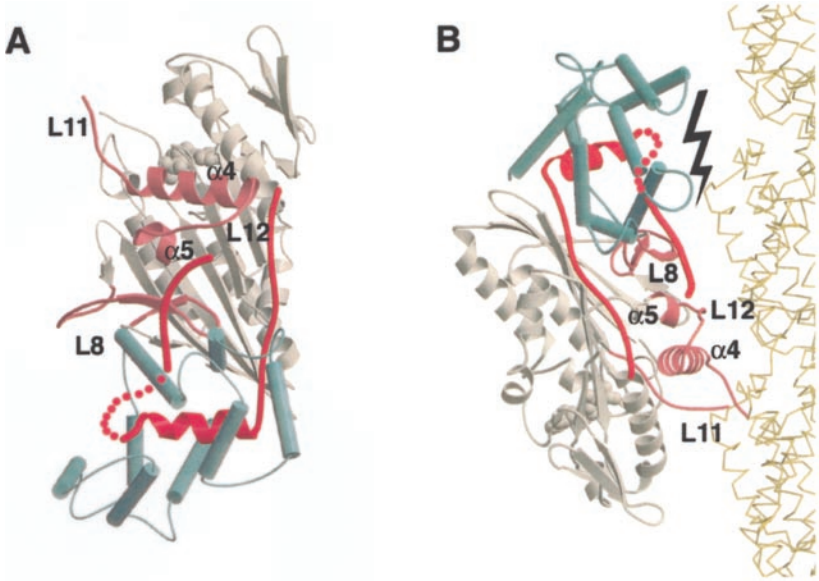

FIG. 3. **Modeling of KCBP-calmodulin complex.** *A*, calmodulin is modeled in the structure of KCBP by superimposing calmodulin-binding motifs on KCBP (residues 1220–1237) and in the structure of calmodulin-binding sMLCK (29) peptide (residues 777–814) complexed with Ca^{2+}-activated calmodulin (PDB entry 1CDL). The KCBP motor core and the bound nucleotide are shown in *gray*, and the regulatory elements are *red*. The major microtubule-binding elements on the motor core are in *pink*. Calmodulin (*steel blue*) is shown as a schematic model. *B*, KCBP-calmodulin complex model positioned on the microtubule. The position of the KCBP motor core is equivalent to that of the AMPPCP-bound kinesin KIF1A docked on the microtubule protofilament (PDB entry 1IA0) (37). The color scheme for the KCBP-calmodulin complex is consistent with *A*. Tubulin subunits of the microtubule protofilament (37) (PDB entry 1IA0) are shown as Cα-carbon tracing *thin wheat-colored lines*. The potential clashes between calmodulin and the microtubule are marked with a *black lightning bolt* symbol.

nucleotide binding pocket is consistent with the previously proposed kinesin-switching mechanism that predicts the pocket will close on binding ATP (32).

DISCUSSION

The Neck Mimic Stabilizes the ATP State of C-terminal Kinesins—Previous studies conclude that a conserved hydrophobic pocket on the surface becomes exposed to solvent when the switch II cluster is in the ATP-like state. In the plus end kinesin dimer, immediate docking of the neck linker along the motor core stabilizes this energetically metastable state. This repositioning of the neck linker culminates in the power stroke of the partner motor head toward the plus end of MTs (33). Because of the different architecture of the neck in the C-terminal kinesins, it was not clear what stabilizes the ATP state of these motors. Finding additional ordered structural segments of KCBP solved the mystery. In the structure of KCBP, the neck mimic stabilizes the ATP-like conformation of the motor (Figs. 1*C* and 2*A*). Fig. 2*A* shows that the KCBP residue Ile^{1210}, which is analogous to the conserved isoleucine residue at the base of the neck linker of conventional kinesin (Ile^{325} in human kinesin (23)), loads into the hydrophobic pocket, thereby facilitating zipping interactions between the neck mimic and the motor core. Notably, all C-terminal kinesins have an extension of at least seven amino acids that are C-terminal to the motor core (4) to which we can now ascribe this function. Furthermore, although not conserved, these neck mimics have one or more hydrophobic residues (Ile^{1210}, Val^{1211}, and Pro^{1214} in KCBP) followed by one or more charged amino acids with extended aliphatic side chains (Lys^{1216} in KCBP). In some C-terminal kinesins (Ncd, KIFC2, and KIFC3 (4)), the neck mimic is followed by a predicted helical region and is likely involved in regulation of these kinesins. In previously reported structures of C-terminal kinesins (22, 25–27) the neck mimic is disordered and therefore not visible, although it is physically present; this is consistent with the observed ADP-bound conformation of these motors. Normally, in C-terminal kinesins the ADP-bound conformation supports the interaction between the core and the true neck and does not support interactions between the core and the neck mimic.

ATP Binding and Minus End-directed Power Stroke—In C-terminal kinesins, ATP binding and associated conformational changes are hypothesized to disrupt the neck core interactions (31, 34). The ATP-stimulated release of the neck that results in the minus end-directed power stroke was recently observed in electron microscopy studies of Ncd (35). The structure of KCBP elaborates the Sablin model for the oppositely directed kinesin power stroke (36) and suggests a detailed mechanism for the ATP-induced neck swing in the minus end-directed kinesins. Comparing the ATP-like structure of KCBP with the ADP-like structure of Ncd (22) shows that the docked ATP-like position of the neck mimic and the docked ADP-like conformation of the true neck cannot coexist (Fig. 4*B*). Isoleucine side chains from these two different chain segments alternately bind in a specialized pocket during ATP hydrolysis. In particular, hydrophobic residues stabilize the position of Ile^{349} at the base of the *docked neck* in the ADP-like structure of Ncd. Analogous hydrophobic residues interact with Ile^{1210} at the base of the *docked neck mimic* in the ATP-like structure of KCBP (Fig. 2*A*). It is clear from Fig. 4*C* that Ile^{890} in the base of the true KCBP neck, the analogue to Ile^{349} of Ncd, is squeezed out of the hydrophobic pocket. Exchange of Ile^{890} for Ile^{1210} causes the β1-strand, which would hold and direct the docked neck in the ADP structure, to bend away (Fig. 4*C*). This reconfiguration of the base of the neck in the ATP-like state of the motor is likely the major destabilizing factor causing the neck to move away from its docked position on the core in ADP-like conformation (Fig. 4*B*). In addition, the ATP-induced docking of the neck mimic would also disable specific, true neck core interactions in the ADP state. For example, the conserved interaction between Asn^{340} and Tyr^{426} at the neck core interface of the ADP-like motor Ncd (22, 31, 34) (equivalent to Asn^{881} and Tyr^{962} in KCBP) would be disrupted. At the same time, the docked neck mimic creates a number of new repelling steric and electrostatic interactions (Fig. 4*C*), which would ensure

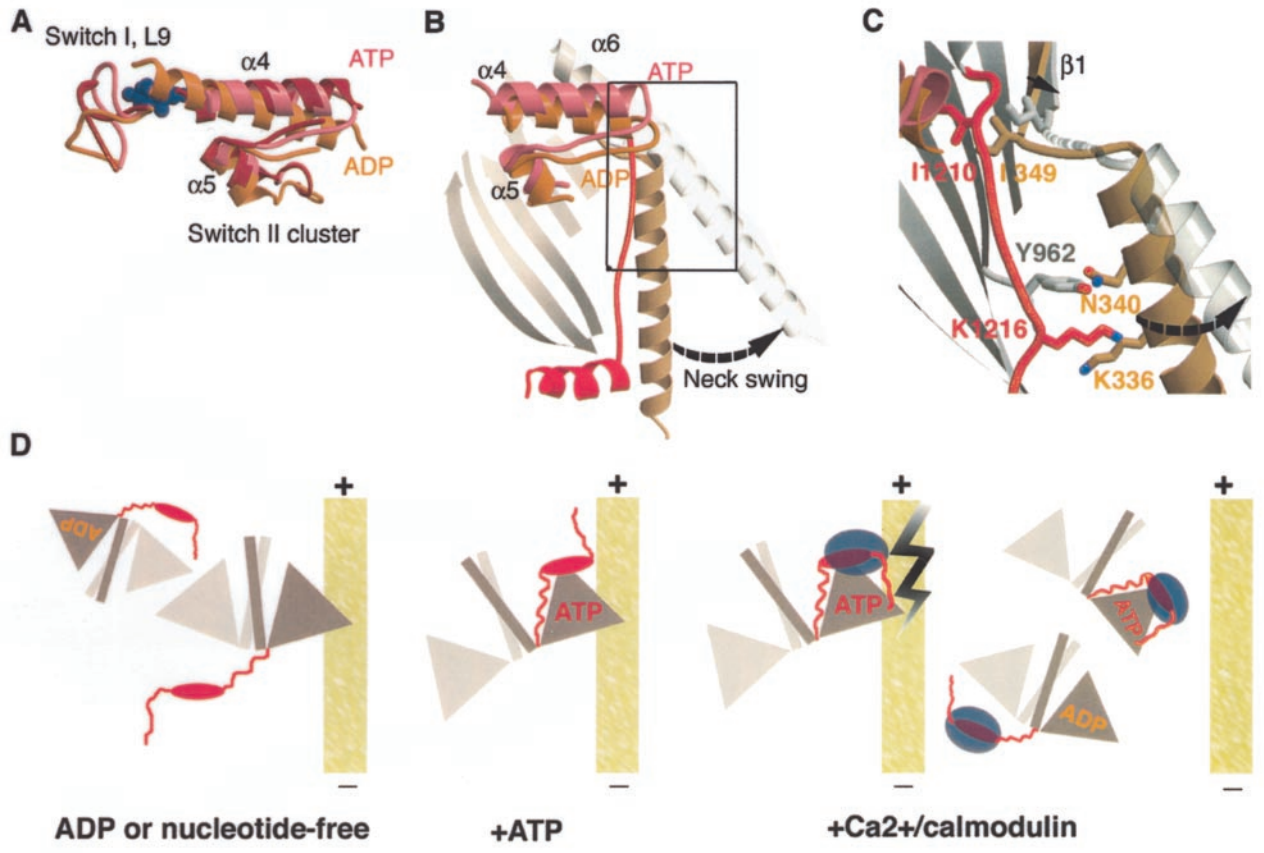

FIG. 4. **Switch-based mechanism of KCBP.** *A*, superimposition of the switch regions of KCBP and ADP- and ATP-like kinesin KIF1A (31) (PDB entries 1I5S and 1I6I, respectively). The superimposed switch I and II regions are shown in *pink*, *red*, and *orange* for KCBP, ATP-, and ADP-like KIF1A, respectively. *B*, two distinct conformations are shown of switch II cluster in the superimposed structures of the ATP-like KCBP (*pink*) and ADP-like Ncd (22) (*orange*) (PDB entry 2NCD). The nucleotide-induced conformational transitions in switch II cluster are transmitted to regulatory and mechanical parts of KCBP. With the neck mimic (*red*) docked along the motor core in the ATP-like state of KCBP, the true neck cannot occupy the same position as in the ADP-like Ncd structure (the Ncd neck is *beige*). The putative new position of the KCBP neck in the ATP-like state is shown as a *transparent ribbon* structure (*rectangular frame* is the enlarged view analyzed in *C*). *C*, specific neck mimic core interactions causing detachment of the neck in the ATP-like state of KCBP. The new switch II cluster conformation results in rearranging hydrophobic residues on the motor core that were previously seen engaged in stabilizing Ile^{349} (Ile^{890} in KCBP) at the base of Ncd neck. The hydrophobic pocket (see Fig. 2*A*) is now occupied by Ile^{1210} of the KCBP neck mimic. Ile^{890} of KCBP, equivalent to Ile^{349} of Ncd, is shown as a stick model but not indicated. All indicated residues causing the repelling interactions are conserved in C-terminal kinesins. *D*, schematic model for the Ca^{2+}-calmodulin regulation of KCBP. KCBP is shown as a functional dimer; the *gray triangle* is the motor core, the *gray* rectangle is the neck, and the regulatory domain is *red*. For simplicity, the partner motor subunit lacks the regulatory domain and has been colored less distinctively. Binding of ATP to the microtubule-attached motor (microtubule is a *yellow-green rectangle*) causes docking of the neck mimic along the motor core. This docking positions the calmodulin-binding helix in the vicinity of the microtubule surface and destabilizes the neck-core interface, pushing the mechanical element of the motor, the neck, away from the motor core. Repositioning of the neck results in the minus end-directed power stroke, which moves the partner motor subunit toward the minus end (−) of the microtubule. When the concentration of Ca^{2+} ions increases, Ca^{2+}-activated calmodulin (*steel blue ellipse object*) binds to the prepositioned calmodulin-binding helix. This binding stabilizes the negative coil, which blocks the microtubule-binding sites of KCBP. The combined effect of calmodulin binding deactivates the motor and causes dissociation of the KCBP-calmodulin complex from the microtubule.

pushing the already destabilized neck away from the core in the ATP-like state. The expelled neck would promote the power stroke as previously suggested (36) (Fig. 4*B*). Thus, similar to ATP-induced docking of the neck linker in the plus end-directed kinesins, the ATP-triggered docking of the neck mimic appears to be the essential part of the force-generating mechanism in the minus end-directed kinesin motors.

Mechanism of Ca^{2+}-Calmodulin Regulation of KCBP—The structure of KCBP suggests a plausible mechanism for Ca^{2+}-calmodulin regulation of kinesins. The neck mimic links the regulatory subdomains of KCBP to the catalytic cycle of the motor. The calmodulin-binding helix is positioned in the vicinity of the KCBP microtubule-binding face in the ATP-like state when interactions between the microtubule track and KCBP are strong. The motor is fully active but sensitized for potential regulatory interactions with calmodulin. A rising concentration of Ca^{2+} activates calmodulin and induces binding it to KCBP. Accessibility of the calmodulin-binding helix while KCBP is bound to the MT allows activated calmodulin to establish the contacts and to block the motility of a working motor. Modeling shows that bound Ca^{2+}-calmodulin would interfere with loop L8 of the KCBP motor core, disabling one of the specific contacts between the kinesin motor and the MT and probably initiating the process of dissociation.

What is the role of the negative segment? Blocking of two major MT-binding elements, loops L8 and L12, in the absence of calmodulin by the negative segment might seem to be a puzzle. Multiple sequence alignment shows that the hyper-negative sequence (^{1242}DDEELEEIQDE^{1252} in KCBP), most of which is visible in the KCBP structure (Fig. 2*C*), is conserved among all plant KCBPs and is, therefore, functionally important; however, MT-binding assays and MT-stimulated ATPase assays with full-length KCBP show that in the absence of Ca^{2+}-calmodulin the negative segment itself does not affect KCBP binding to MTs (8, 9, 14). Only in the presence of calmodulin is the negative segment able to compete with the more

extensive, negatively charged surface of the MT. Therefore, we suggest that the conformation of the negative segment observed in the KCBP structure is functionally relevant and likely corresponds to the conformation of the protein in the complex with calmodulin. In addition to directly blocking the microtubule-binding elements of the motor (Fig. 3*B*), calmodulin would help to order the negative segment and fix it as observed.

Calmodulin regulates the functions of numerous structurally and functionally diverse proteins. The modes of calmodulin binding vary to respond to the specific requirements of regulation and could be different between protein and peptide targets (30). The model discussed here allowed us to explain the biochemistry of KCBP and suggests the plausible mechanism of regulation of kinesin motors by Ca^{2+}-calmodulin; however, the atomic resolution structure of the KCBP-Ca^{2+}-calmodulin complex is needed to test the suggested regulatory mechanism.

Conclusions—It is an engineering marvel that the switching mechanism can be used by kinesins for generating motility and in their regulation. In the case of KCBP, the nucleotide-sensing switch regions coordinate functions of mechanical and regulatory domains. Zipping of the neck mimic along the motor core stabilizes the ATP-like state of the C-terminal KCBP core, simultaneously pushing its mechanical element, the neck, toward the minus end of the MT and also properly orienting the regulatory calmodulin-binding helix (Fig. 4*D*). When Ca^{2+}-activated calmodulin binds to KCBP, it deactivates the motor by blocking the microtubule-binding elements on the motor core, resulting in dissociation of the complex from the microtubule. The negative regulation of KCBP by calmodulin is reinforced by the repelling electrostatic interactions between the KCBP-calmodulin complex and the track because of the calmodulin-assisted attachment of the KCBP negative coil on the microtubule-binding sites of the motor.

Acknowledgments—We thank Irene Day for comments on the manuscript and James Holton and the Advanced Light Source 8.3.1.beamline staff for excellent technical support.

REFERENCES

1. Chin, D., Means, A. R. (2000) *Trends Cell Biol.* **10,** 322–328
2. Espindola, F.S., Suter, D.M., Partata, L.B., Cao, T., Wolenski, J.S., Cheney, R.E., King, S.M., Mooseker, M.S (2000) *Cell Motil. Cytoskeleton* **47,** 269–281
3. Casey, D.M., Inaba, K., Pazour, G.J., Takada, S., Wakabayashi, K., Wilkerson, C.G., Kamiya, R., Witman, G.B. (2003) *Mol. Biol. Cell* **14,** 3650–3663
4. Hirokawa, N. (1998) *Science* **279,** 519–526
5. Vale, R. D. (2003) *Cell* **112,** 467–480
6. Reddy, A. S. N., and Day, I. S. (2001) *BMC Genomics* **2,** 2–12
7. Reddy, A. S. N. (2001) *Int. Rev. Cytol.* **204,** 97–178
8. Song, H., Golovkin, M., Reddy, A. S. N., and Endow, S. A. (1997) *Proc. Natl. Acad. Sci. U. S. A.* **94,** 322–327
9. Reddy, A. S. N., Narasimhulu, S. B., Safadi, F., and Golovkin, M. (1996) *Plant J.* **10,** 9–21
10. Rogers, G. C., Hart, C. L., Wedman, K. P., and Scholey, J. M. (1999) *J. Mol. Biol.* **294,** 1–8
11. Bowser, J., and Reddy, A. S. N. (1997) *Plant J.* **12,** 1429–1437
12. Vos, J. W., Safadi, F., Reddy, A. S. N., and Hepler, P. K. (2000) *Plant Cell* **12,** 979–990
13. Oppenheimer, D. G., Pollock, M. A., Vacik, J., Szymanski, D. B., Ericson, B., Feldmann, K., Marks, M. D. (1997) *Proc. Natl. Acad. Sci. U. S. A.* **94,** 6261–6266
14. Deavours, B. E., Reddy, A. S. N., and Walker, R. A. (1998) *Cell Motil. Cytoskeleton* **40,** 408–416
15. Kao, Y. L., Deavours, B. E., Phelps, K. K., Walker, R. A., and Reddy, A. S. N. (2000) *Biochem. Biophys. Res. Commun.* **267,** 201–207
16. Reddy, A. S. N., Safadi, F., Narasimhulu, S. B., Golovkin, M., and Hu, X. (1996) *J. Biol. Chem.* **271,** 7052–7060
17. Reddy, V. S., and Reddy, A. S. N. (2002) *J. Biol. Chem.* **277,** 48058–48065
18. Otwinowski, Z., and Minor, W. (1997) *Methods Enzymol.* **276,** 307–326
19. Brunger, A. T., Adams, P. D., Clore, G. M., DeLano, W. L., Gros, P., Grosse-Kunstleve, R. W., Jiang, J. S., Kuszewski, J., Nilges, M., Pannu, N. S., Read, R. J., Rice, L. M., Simonson, T., Warren, G. L. (1998) *Acta Crystallogr. Sect. D Biol. Crystallogr.* **54**, 905–921
20. Collaborative Computational Project, Number 4 (1994) *Acta Crystallogr. Sect. D Biol. Crystallogr.* **50**, 760–763
21. Kull, F. J., Sablin, E. P., Lau, R., Fletterick, R. J., and Vale, R. D. (1996) *Nature*, **380,** 550–555
22. Sablin, E. P., Case, R. B., Dai, S. C., Hart, C. L., Ruby, A., Vale, R. D., Fletterick, R. J. (1998) *Nature*, **395,** 813–816
23. Sindelar, C. V., Budny, M. J., Rice, S., Naber, N., Fletterick, R., Cooke, R. (2002) *Nat. Struct. Biol.* **9,** 844–848
24. Kozielski, F., Sack, S., Marx, A., Thormahlen, M., Schonbrunn, E., Biou, V., Thompson, A., Mandelkow, E. M., Mandelkow, E. (1997) *Cell* **91,** 985–994
25. Gulick, A. M., Song, H., Endow, S. A., and Rayment, I. (1998) *Biochemistry* **37,** 1769–1776
26. Yun, M., Zhang, X., Park, C. G., Park, H. W., and Endow, S. A. (2001) *EMBO J.* **20,** 2611–2618
27. Yun, M., Bronner, C. E., Park, C. G., Cha, S. S., Park, H. W., Endow, S. A.. (2003) *EMBO J.* **22,** 5382–5389
28. Sosa, H., Dias, D. P., Hoenger, A., Whittaker, M., Wilson-Kubalek, E., Sablin, E., Fletterick, R. J., Vale, R. D., Milligan, R. A. (1997) *Cell*, **90,** 217–224
29. Meador, W. E., Means, A. R., and Quiocho, F. A. (1992) *Science*, **257,** 1251–1255
30. Vetter, S. W., and Leclerc, E. (2003) *Eur. J. Biochem.* **270,** 404–414
31. Kikkawa, M., Sablin, E. P., Okada, Y., Yajima, H., Fletterick, R. J., Hirokawa, N. (2001) *Nature*, **411,** 439–445
32. Naber, N., Naber, N., Minehardt, T. J., Rice, S., Chen, X., Grammer, J., Matuska, M., Vale, R. D., Kollman, P. A., Car, R., Yount, R. G., Cooke, R., Pate, E. (2003) *Science*, **300,** 798–801
33. Rice, S., Rice, S., Lin, A.W., Safer, D., Hart, C. L., Naber, N., Carragher, B. O., Cain, S. M., Pechatnikova, E., Wilson-Kubalek, E. M., Whittaker, M., Pate, E., Cooke, R., Taylor, E. W., Milligan, R. A., Vale, R. D. (1999) *Nature*, **402,** 778–784
34. Sablin, E. P., and Fletterick, R. J. (2001) *Curr. Opin. Struct. Biol.* **1,** 716–724
35. Wendt, T. G., Volkmann, N., Skiniotis, G., Goldie, K. N., Muller, J., Mandelkow, E., Hoenger, A. (2002) *EMBO J.* **21,** 5969–5978
36. Sablin, E. P., Kull, F. J., Cooke, R., Vale, R. D., Fletterick, R. J. (1996) *Nature* **380,** 555–559
37. Kikkawa, M., Okada, Y., and Hirokawa, N. (2000) *Cell* **100,** 241–252